

Claudin-8 Expression in Madin-Darby Canine Kidney Cells Augments the Paracellular Barrier to Cation Permeation*

Received for publication, December 31, 2002, and in revised form, February 20, 2003
Published, JBC Papers in Press, March 2, 2003, DOI 10.1074/jbc.M213286200

Alan S. L. Yu^{‡§}, Alissa H. Enck[¶], Wayne I. Lencer^{||}, and Eveline E. Schneeberger^{**}

From the [‡]Division of Nephrology, Department of Medicine, and Department of Physiology and Biophysics, University of Southern California Keck School of Medicine, Los Angeles, California 90033, [¶]Renal Division, Brigham and Women's Hospital, Boston, Massachusetts 02115, ^{**}Department of Pathology, Massachusetts General Hospital, Boston, Massachusetts 02114, and ^{||}Gastrointestinal Cell Biology, Department of Pediatrics, Children's Hospital and Harvard Digestive Diseases Center, Boston, Massachusetts 02115

Claudins are a family of integral membrane proteins of the tight junction that are thought to participate in the permeation of solutes across epithelia via the paracellular pathway. Claudin-8 is expressed in the distal renal tubule, which has a characteristically low passive permeability to monovalent cations. To test the hypothesis that claudin-8 plays a role in forming a tight paracellular barrier to cations, stably transfected Madin-Darby canine kidney II cell lines with inducible expression of claudin-8 were generated. Induction of claudin-8 expression was associated with down-regulation of endogenous claudin-2 protein. Other tight junction proteins were expressed and targeted normally, and the number of junctional strands was minimally altered. By Ussing chamber and radiotracer flux studies, claudin-8 expression was found to reduce paracellular permeability to monovalent inorganic and organic cations and to divalent cations but not to anions or neutral solutes. The size selectivity, charge dependence, and activation energy of paracellular cation permeation were all unchanged. These observations are consistent with a model in which claudin-2 encodes a highly cation-permeable channel, whereas claudin-8 acts primarily as a cation barrier. When exogenous claudin-8 is expressed, it replaces endogenous claudin-2, inserting in its place into existing tight junction strands, thereby reducing the apparent number of functional cation pores. Our findings suggest that claudin-8 plays an important role in the paracellular cation barrier of the distal renal tubule.

Vectorial transport across epithelia can occur via the transcellular or paracellular route. The molecular basis of transcellular transport, mediated by proteins that catalyze transmembrane movement of solutes and water at the apical and basolateral surfaces, is well understood. By contrast, little is known about the mechanisms of paracellular transport. The tight junction, which is the most apical of the intercellular

junctional complexes at the lateral membrane, is generally believed to be the rate-limiting step in paracellular transport. The tight junction is composed of a complex of multiple proteins, many of uncertain function (1, 2). Most of these proteins are cytoplasmic in location, and several are associated with the cytoskeleton via the perijunctional actin ring. In recent years, a number of integral membrane proteins associated with the tight junction have been identified, including occludin (3), junction-associated membrane proteins 1 and 2 (4, 5), Coxsackie- and adenovirus-associated receptor (6), 1G8 antigen (7), and the claudins (8). Integral membrane proteins are of particular interest because, by definition, their extracellular domains must protrude into the lateral intercellular space and, therefore, may potentially have direct contact with solutes as they permeate through the paracellular pathway.

Claudins are the most heterogeneous of these integral membrane proteins and consist of a family of at least 20 homologous isoforms (9). Moreover, each isoform clearly exhibits a tissue-specific and segment-specific pattern of distribution in epithelia such as those of the gastrointestinal tract (10) and renal tubule (11–13). Claudins are therefore leading candidates for the molecular determinants responsible for the variety of different paracellular permeability properties found in different epithelia. Several recent reports provide convincing evidence that claudins regulate paracellular permeability. Human mutations in claudin-16 cause failure of paracellular reabsorption of divalent cations in the thick ascending limb of the renal tubule, leading to familial hypercalciuric hypomagnesemia (14), and a preliminary report suggests that knockout mice lacking claudin-16 may have a similar phenotype (15). Both claudin-1-deficient mice (16) and transgenic mice overexpressing claudin-6 (17) exhibit abnormally high epidermal permeability to water. Overexpression of claudins 1, 4, and 15 in MDCK¹ cells all increase transepithelial resistance (TER) (18–21), whereas overexpression of claudin-2 markedly decreases TER (22) by selectively increasing permeability to cations (23). Furthermore, Anderson and co-workers (20, 21) elegantly show that, although overexpression of claudin-4 reduces paracellular monovalent cation permeability, this can be abolished by altering the net charge at the first extracellular loop by site-directed mutagenesis. Similarly, although claudin-15 alone does not alter the relative preference of the paracellular pathway between Na⁺ and Cl⁻, mutating anionic extracellular residues to cationic ones makes the paracellular pathway more anion-selective (21).

Thus, the contention that claudins have a direct role in

* This work was supported by a Satellite Healthcare Extramural Research Grant (to A. S. L. Y.) and by National Institutes of Health Grants HL25822 (to E. E. S.), DK34854 (to the Harvard Digestive Diseases Center), and DK48522 (to the University of Southern California Center for Liver Diseases for the Microscopy Sub-core). The costs of publication of this article were defrayed in part by the payment of page charges. This article must therefore be hereby marked "advertisement" in accordance with 18 U.S.C. Section 1734 solely to indicate this fact.

§ To whom correspondence should be addressed: University of Southern California Keck School of Medicine, Div. of Nephrology, 2025 Zonal Ave., RMR 406, Los Angeles, CA 90033. Tel.: 323-442-1331; Fax: 323-442-3093; E-mail: alanyu@usc.edu.

¹ The abbreviations used are: MDCK cells, Madin-Darby canine kidney cells; TER, transepithelial resistance; Dox, doxycycline.

regulating the magnitude and nature of paracellular permeability is now irrefutable. However, the plethora of published claudin overexpression and gene ablation experiments has uncovered a fundamental paradox. Claudin overexpression can be associated with both an increase (17, 22, 23) and a decrease (18–21) in paracellular permeability; similarly, knockout or inactivating mutations of claudin genes can cause either an increase (16) or a decrease (14, 15) in paracellular permeability. Thus, in the absence of suitable models to explain such contradictory observations, attempts to infer the permeability properties of specific claudin isoforms remain problematic.

A possible solution emerges if one views each tight junction strand as a continuous string of protein molecules (such as claudins, occludin, or other proteins) arrayed side-by-side, rather like beads on a necklace, so as to form an uninterrupted seal (9). In such a model, claudins would play a bipartite role, acting as a barrier by sealing the gaps between protein particles, and simultaneously providing a channel through that barrier from the apical compartment to the lateral intercellular space. This may explain why the complete loss of a claudin isoform can have diametrically opposite consequences. In the absence of any changes in other tight junction proteins, gaps would appear in the continuous seal, and the paracellular route would become more permeable. Conversely, when other components of the tight junction become up-regulated and fill in for the absent claudins, the paracellular route may become less permeable. Similar considerations may govern the consequences of overexpression experiments. The resulting phenotype is complex and dependent on the properties both of the heterologously expressed claudin and of endogenous tight junction proteins.

In this manuscript, we describe a new tissue culture model with overexpression of claudin-8. We chose to study claudin-8 because previous *in situ* hybridization (11) and immunohistochemical studies (12) revealed that it is expressed primarily in the aldosterone-sensitive distal nephron. In these segments of the renal tubule, the paracellular barrier is particularly tight to monovalent cations and protects transtubular gradients up to 1000:1 for H⁺, 20:1 for K⁺, and 1:3 for Na⁺. We therefore tested the hypothesis that claudin-8 plays a role in impeding paracellular cation permeation. We show that the combination of careful biochemical, histological, and physiological studies constitute a powerful tool to interpret the phenotype of such overexpression experiments. We propose potential models to explain the findings of such studies and show data that indicate that claudin-8 acts as a nonspecific cation barrier.

MATERIALS AND METHODS

Generation of MDCK II TetOff Claudin-8 NFL Cell Lines—A 675-bp DNA fragment containing the mouse claudin-8 coding sequence except for the initiation codon was amplified by PCR from a cDNA clone (IMAGE ID: 162549) and inserted into a FLAG epitope tag shuttle vector based on pcDNA3 (24) so that the claudin-8 N terminus was fused in-frame with a sequence encoding MDYKDDDDKGS (the FLAG octapeptide tag is underlined followed by a glycine-serine linker encoding *Bam*HI restriction site). The entire coding region was then excised and cloned into the retroviral Tet response vector, pRevTRE (Clontech, Palo Alto, CA) to obtain the plasmid, pRev-mCLDN8-NFL. Plasmid DNA was transfected by lipofection into the packaging cell line, PT67, a polyclonal culture of stable transfectants selected using hygromycin, and virus-containing supernatant collected from the growth medium. MDCK II TetOff cells expressing the tetracycline-regulated transactivator from a cytomegalovirus promoter (Clontech) were infected with viral supernatant in the presence of Polybrene. Stable transfectants were selected by growth in 0.3 mg/ml hygromycin. Clonal cell lines were isolated using plastic cloning rings and three clones (2, 4, and 9) with strong induction of claudin-8 expression (see “Results”) used for further studies. Cells were maintained in Dulbecco’s modified Eagle’s medium with 5% fetal bovine serum, 0.1 mg/ml G418, 0.3 mg/ml hygromycin, and 20 ng/ml doxycycline (Dox+). To induce claudin-8 expression, doxy-

cline was omitted from the culture medium starting from the day of plating (Dox−). Studies were generally performed after 4–6 days except where otherwise indicated.

Detection of Tight Junction Proteins by Immunoblot and Immunohistochemistry—To detect tight junction protein expression by immunoblotting, cultured cells were first homogenized and fractionated by centrifugation at 100,000 × *g* as described previously (24). No claudin-8 was ever detectable in the soluble fraction (100,000 × *g* supernatant). The total amount of protein isolated from plates of confluent Dox+ and Dox− cells was similar, and the fractional yield of membrane protein (100,000 × *g* pellet) was roughly 15% in both. Aliquots of 25 μg of membrane protein were then electrophoresed on denaturing SDS-polyacrylamide gels and transferred to polyvinylidene difluoride membrane, and Western blots were performed using the ECL chemiluminescence kit (Amersham Biosciences). Claudin-8 transgene expression was detected with the M2 anti-FLAG monoclonal antibody (Sigma) at a 1:400 dilution. Antibodies to ZO1, occludin, and claudins 1–4 were obtained from Zymed Laboratories Inc., San Francisco, CA and used at the concentrations recommended by the manufacturer. Rabbit anti-Coxsackie- and adenovirus-associated receptor antiserum (a kind gift of Dr. Christopher Cohen, Children’s Hospital of Philadelphia, PA) was used at 1:5000 dilution. Western blots were digitized with a flatbed optical scanner. Gray scale values were logarithmically transformed to obtain uncalibrated optical density estimates, and individual bands were quantitated using NIH Image 1.61 software (rsb.info.nih.gov/nih-image).

To determine the localization of claudin-8 protein expression, cell lines grown on 12-mm Transwell-Clear polyester filters (1-cm² growth area, 0.4-μm pore size; Corning Costar, Acton, MA) were fixed with 4% paraformaldehyde at 4 °C for 15 min, then indirect immunofluorescence staining was performed either with the M2 mouse antibody at 1:400 dilution or (for the double labeling study shown in Fig. 1C) with a rabbit anti-claudin-8 antibody (933) at 1:100 dilution, all in the presence of 0.3% Triton X-100 using protocols described previously (24). Affinity-purified rabbit polyclonal antibody 933 was raised against the claudin-8 C-terminal peptide, CQRSFHAEKRSPIYSKSYQV (25). Images were acquired at the University of Southern California Center for Liver Diseases using a Nikon PCM confocal microscopy system with argon and helium-neon lasers.

Freeze Fracture and Immunolabeling—Freeze fracture with or without immunolabeling was performed essentially as described previously (19). Confluent monolayers were fixed either in 2% glutaraldehyde at 4 °C for 30 min (no immunolabeling) or in 1% paraformaldehyde at 4 °C for 15 min (for immunolabeling). They were then rinsed in phosphate-buffered saline, scraped from the filter, and infiltrated with 25% glycerol in 0.1 M cacodylate buffer for 60 min at 4 °C. Cell pellets were frozen in liquid nitrogen slush, and freeze-fractured at −115 °C in a Balzers 400 freeze-fracture unit (Lichtenstein). Processing of the replicas for strand morphometry and immunolabeling was as described (26), and the replicas were examined with a Philips 301 electron microscope. The number of parallel strands in the tight junctions was quantified as described previously (26). Because the frequency distribution of strand number was non-Gaussian, the difference in the median number of strands in Dox+ and Dox− cells was assessed for statistical significance using the Wilcoxon ranked sum test. Immunolabeling of SDS-treated replicas was performed with the M2 anti-FLAG antibody (1:100) followed by goat anti-mouse gold (1:100).

TER Monitoring—Cells were plated at confluent density (2 × 10⁵ cells/cm²) onto Transwell filters loaded in 12-well plates. The resistance across each filter in culture media was measured at room temperature by immersing into the well chopstick-style Ag/AgCl electrodes attached to a Millicell-ERS voltohmmeter (Millipore, Bedford, MA). TER was calculated by subtracting the resistance determined in blank filters from the resistance measured in filters with monolayers.

Ussing Chamber Electrophysiology Studies—Cells were plated at confluent density on 1 cm² Snapwell polyester filters (Corning Costar) and grown for the indicated number of days. The filter rings were then detached and mounted in Ussing chambers that were incubated in Ringer solution (150 mM NaCl, 2 mM CaCl₂, 1 mM MgCl₂, 10 mM glucose, 10 mM HEPES, pH 7.4) at 37 °C and continuously bubbled with 95% O₂, 5% CO₂. The fluid volume on each side of the filter was 4 ml. Voltage-sensing electrodes consisting of Ag/AgCl pellets and current-passing electrodes of silver wire were connected by agar bridges containing 3 M KCl and interfaced via head-stage amplifiers to a microcomputer-controlled voltage/current clamp (DM-MC6 and VCC-MC6, respectively; Physiologic Instruments, San Diego, CA).

Voltage-sensing electrodes were matched to within 1 mV asymmetry and corrected by an offset-removal circuit. The voltage between the two

compartments (values reported are referenced to the apical side) was monitored and recorded at 5-s intervals, whereas the current was continuously clamped to zero. This was done to minimize current-induced local changes of salt concentration in the unstirred layers, which can generate spontaneous potentials due to the transport-number effect (27). The voltage was first measured with blank filters in each combination of buffers to be used for the experiments. The values obtained, which were generally less than 1 mV in magnitude, represent the difference in junction potentials between the two voltage-sensing bridges summed with any potential that might exist across the filter membrane. These were subtracted from all subsequent measurements with filters containing attached cell monolayers to determine transepithelial voltage (V_e).

The total resistance between apical and basal compartments was determined in Ringer at the start and at intervals throughout the experiment from the voltage evoked by a 5- μ A bipolar current pulse. The background resistance determined with blank filters (62.0 ± 1.0 ohm, $n = 6$), representing the sum of the resistances of the filter, of the fluid in the chambers and of the current-passing electrodes and bridges was subtracted from the total resistance measured with filters containing attached cell monolayers to determine the TER and hence conductance (TER^{-1}). TER was found to be maintained within 5% of its baseline value for at least 2 h, whereas the duration of an experiment was typically about 60–90 min.

Dilution and biionic potentials were determined by replacing the solution of one compartment, generally the basal side to minimize flow disruption of the integrity of the monolayer, while keeping the other side bathed in Ringer. In selected cases the solution in the apical compartment was replaced instead of the basal side and showed identical results (see for example Fig. 5B). For 2:1 NaCl dilution potentials, the 150 mM NaCl in Ringer was replaced with 75 mM NaCl, and the osmolality was maintained with mannitol. For biionic potentials, 150 mM NaCl was replaced with 150 mM chloride salt of the indicated alkali metal or organic cation. Organic cations that were obtained as free amine compounds were titrated to neutrality with HCl to form the chloride salt. All organic cations used had a pK_a greater than 9.0; therefore, they were all assumed to be completely protonated at pH 7.4. In biionic potential experiments using near-impermeant organic cations, contamination of the solution with residual traces of Na^+ could lead to a significant overestimation of the permeability (28). To exclude this, multiple washes with Na^+ -free, organic cation-containing buffer were performed. A "bracketed" protocol was used in which each measurement in asymmetrical salt solutions was both preceded and followed by measurements in symmetrical Ringer to control for any time-dependent variation in the properties of the monolayer and for "memory" effects on the liquid junction potential (29).

Radioactive Tracer Flux Studies—Transmonolayer [^3H]mannitol, [^{14}C]urea, and [^{45}Ca] tracer flux studies were performed by a modification of the method described by McCarthy *et al.* (19). Studies were performed in 12-well plates of Transwell filters in culture medium that already contained 1.8 mM Ca^{2+} . For mannitol and urea assays, 1 mM unlabeled substrate was also added to the medium in both compartments. Flux studies were initiated by adding 1–4 $\mu\text{Ci/ml}$ of the appropriate radioisotope (specific activity, 1–2 Ci/mol) to one side (*cis* compartment) followed by incubation at 37 °C. At 30-min intervals, 100 μl of medium was collected from the *trans* compartment for liquid scintillation counting and replaced with an equal volume of fresh medium at 37 °C. Tracer accumulation for all three solutes was found to be linear from 30 to 60 min, and this was used to determine the flux rate and, hence, total permeability, P_{Tot} . To correct for the effect of the filter membrane and adjacent unstirred layers, the tracer permeability across blank filters, P_{Blank} , was determined concurrently. Transepithelial permeability, P_{TE} , was then calculated from the following equation.

$$P_{\text{TE}} = [(1/P_{\text{Tot}}) - (1/P_{\text{Blank}})]^{-1} \quad (\text{Eq. 1})$$

Statistical Analysis and Mathematical Modeling—Data are presented as the means \pm S.E., where n indicates the number of monolayers from a single experiment. Differences between groups were assessed for statistical significance using the unpaired two-tailed Student's t test. Nonlinear regression analyses were performed by the Levenberg-Marquardt method using GraphPad Prism 3 software. All results shown are representative of at least three separate experiments unless otherwise indicated.

The relative ionic permeabilities of the monolayers were calculated using the Goldman-Hodgkin-Katz equation. This is justified because the equation was shown to fit our data well (see "Results" and Fig. 5). The individual permeabilities to Na^+ (P_{Na}) and Cl^- (P_{Cl}) in symmetrical

150 mM NaCl were deduced from the method of Kimizuka and Koketsu (30) using the following equations,

$$P_{\text{Na}} = G \cdot (RT/F^2)/(a(1 + \beta)) \quad (\text{Eq. 2})$$

$$P_{\text{Cl}} = P_{\text{Na}} \cdot \beta \quad (\text{Eq. 3})$$

where G is the conductance per unit surface area, a is the NaCl activity, and β is the ratio of the permeability of Cl^- to that of Na^+ as determined by the Goldman-Hodgkin-Katz equation. All calculations used activities rather than concentrations. The mean activity coefficient of each monovalent cation-halide salt was assumed to be the same as that of NaCl, and the anion and cation in each case were assumed to have the same activity coefficient (Guggenheim assumption).

RESULTS

Generation of Cell Lines with Inducible Claudin-8 Expression at the Tight Junction—To investigate the role of claudin-8 in paracellular permeability, we first generated cell lines overexpressing the claudin-8 protein. We first ascertained by low stringency Northern blot analysis that the canine renal tubule epithelial cell line, MDCK II, does not express claudin-8 endogenously (data not shown). We then generated by retroviral transduction three MDCK II clonal cell lines with stable heterologous expression of N-terminal FLAG epitope-tagged claudin-8 under the control of the TetOff system. Claudin-8 expression was induced in these cells by omitting doxycycline from the medium (Dox $-$) and suppressed by adding doxycycline (Dox $+$). By Western blotting and by immunohistochemistry using the FLAG antibody, claudin-8 protein was found to be expressed in Dox $-$ cells but was completely undetectable in Dox $+$ cells (Fig. 1, A and B). By immunohistochemistry, claudin-8 in confluent Dox $-$ cell monolayers was expressed at the apical end of the lateral cell membrane, where the tight junction is located, and colocalized with the tight junction scaffolding protein, ZO1 (Fig. 1C). On electron microscopic examination of freeze fracture images, the number of tight junction strands appeared similar (Fig. 2, A and B). Careful quantitative morphometry (Fig. 2C) revealed a small but statistically significant increase in strand number (median 4 in Dox $-$ cells, 3 in Dox $+$, $p < 0.0001$). Tight junction morphology was mostly normal, although we observed rare short, disconnected strands in Dox $-$ cells that were never found in Dox $+$ cells. By freeze-fracture immunogold labeling, we confirmed that claudin-8 is incorporated into the tight junction strands (Fig. 2, A and B). This indicates that claudin-8 was appropriately targeted to the tight junction and that the presence of an epitope tag at the N terminus did not interfere significantly with this process.

To ascertain the integrity of the tight junction, the quantity and localization of other proteins known to be present in tight junctions of MDCK II cells were assessed by Western blotting with scanning densitometry and by immunohistochemistry. The expression levels of ZO1, occludin, coxsackie- and adenovirus-associated receptor, and claudins 1, 3, and 4 were not significantly different between Dox $-$ and Dox $+$ cells, and their patterns of localization to the lateral membrane were all identical (Fig. 3). However, by Western blotting, claudin-2 expression in Dox $-$ cells was found to be decreased by $66 \pm 5\%$ ($n = 3$ different clones) compared with Dox $+$ cells (Fig. 3A), and immunofluorescence staining for claudin-2 at the tight junction was qualitatively observed to also be attenuated (Fig. 3B).

Effect of Claudin-8 on Paracellular Electrical Resistance—MDCK II cells are normally moderately leaky with TERs of 50–100 $\text{ohm}\cdot\text{cm}^2$ (31). Thus, the TER is dominated by the resistance of the paracellular pathway and is a useful measure of its permeability to small ions (predominantly Na^+ , as will be shown below). MDCK II cells plated at confluent density on microporous filters exhibit a brisk increase in TER that peaks at 24–72 h and then declines to a steady-state base line over

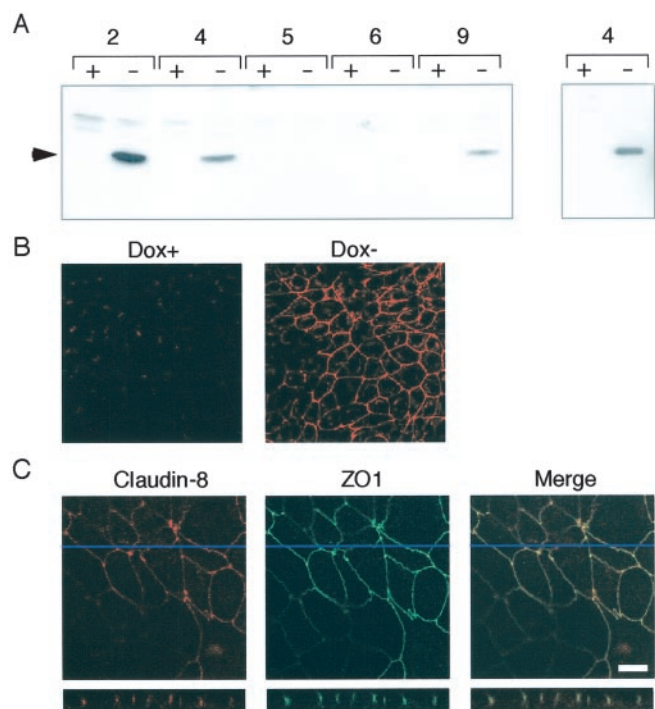


FIG. 1. Characterization of MDCK II TetOff cell lines stably transfected with claudin-8-FLAG and grown in the presence (+) or absence (-) of doxycycline to suppress or induce expression from the Tet promoter, respectively. *A*, left panel, Western blot with FLAG antibody of 100,000 \times *g* membrane fractions (25 μ g of protein/lane) isolated from 5 independent clones cultured on plastic dishes. An inducible band of the expected size for the claudin-8 polypeptide (25 kDa, arrowhead) is observed in clones 2, 4, and 9. Right panel, duplicate blot of clone 4, cultured on permeable filter support. *B*, immunofluorescence staining of claudin-8 in confluent Dox+ and Dox- monolayers with FLAG antibody. *C*, confocal micrographs of a Dox- monolayer double-stained with rabbit claudin-8 antibody (red channel) and mouse ZO1 antibody (green channel). Upper panels, en face images at the level of the tight junction. Lower panels, vertical sections reconstructed in the plane indicated by the blue line. The white scale bar represents 10 μ m. Note claudin-8 staining at the apical end of the intercellular junction, where it completely colocalizes with ZO1 (yellow on the merged images).

5–7 days (Fig. 4, A–B). In Dox- cells, both the peak TER of the initial overshoot and the steady-state TER were increased relative to Dox+ cells. Qualitatively similar results were observed in all three clones but not in control untransfected MDCK II TetOff cells (Fig. 4, C and D). These findings suggest that exogenous claudin-8 expression enhances the paracellular barrier to charged ions and augments this barrier function further during periods of tight junction assembly.

Paracellular Permeability to Na^+ and Cl^- —To determine the identity and quantitative contribution of the ion(s) carrying the paracellular current and the electrophysiological basis for the differences induced by expression of claudin-8, monolayers of the transfected cell lines were mounted in Ussing chambers, and transepithelial voltage and conductance were monitored under current-clamp conditions. As shown in Fig. 5A, imposition of a 2:1 concentration gradient of NaCl from apical to basal side induced a potential difference of -14.1 ± 0.3 mV (apical negative), indicating that the monolayer is more permeable to Na^+ than to Cl^- , as has been established by previous investigators (20, 31, 32). The magnitude of this dilution potential was reduced in Dox- cells (-5.3 ± 0.5 mV; $p < 0.0005$, $n = 3$), indicating that the ratio between the permeability to Na^+ and that to Cl^- ($P_{\text{Na}}/P_{\text{Cl}}$) was decreased. Upon imposing varying NaCl concentration gradients in both directions, the dilution potentials were observed to vary in a manner

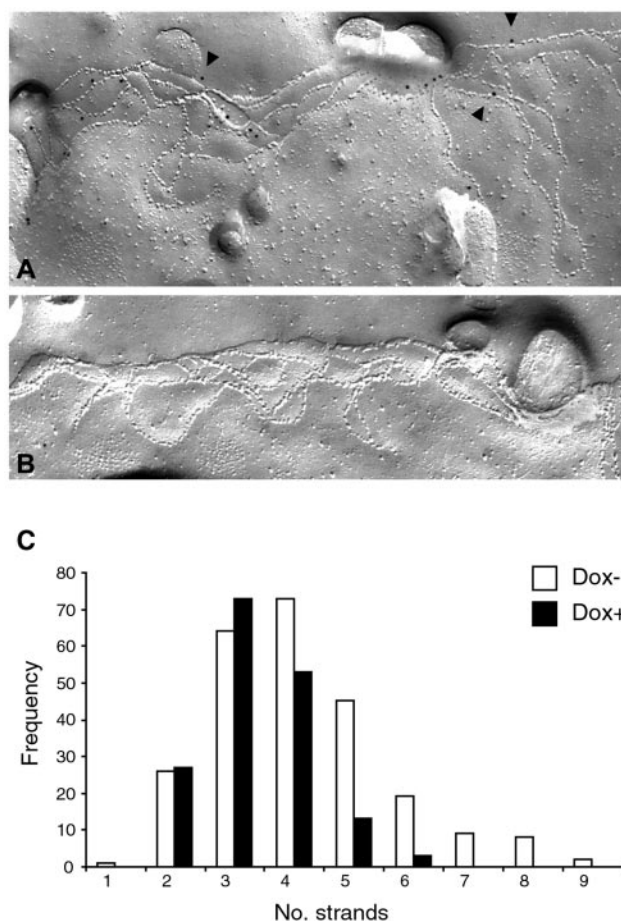


FIG. 2. Fracture-labeled replicas of claudin-8-FLAG-transfected MDCK II cells cultured for 5 days (A) without or (B) with Dox. *A*, monoclonal anti-FLAG antibody sparsely, but specifically, labels tight junction strands in Dox- cell monolayers that express FLAG-tagged claudin-8 (representative gold particles are indicated by arrowheads). *B*, no labeling is detected in Dox+ cell monolayers. Magnification, $\times 62,500$. *C*, frequency histogram showing tight junction strand counts performed at 210 nm intervals in Dox- (white columns) and Dox+ (black columns) cells.

that conformed closely to the Goldman-Hodgkin-Katz equation, at least up to a 3-fold concentration gradient (Fig. 5B). The Goldman-Hodgkin-Katz equation has previously been shown to be a reasonable model to approximate the behavior of other leaky epithelia despite the fact that the assumption of a constant field is likely to be incorrect (33). This equation was therefore used to derive quantitative estimates for $P_{\text{Na}}/P_{\text{Cl}}$. Furthermore, from the total conductance measured in 150 mM NaCl, the absolute values of P_{Na} and P_{Cl} could be deduced. Induction of claudin-8 expression was found to be associated with a 70% reduction in P_{Na} ($p < 0.0005$), whereas P_{Cl} did not change (Fig. 5C). These findings suggest that claudin-8 augments the paracellular barrier to Na^+ permeation. Fig. 5D summarizes the results of multiple measurements performed on monolayers at different time points after plating. This shows that the conductance of the monolayer was linearly related to P_{Na} , demonstrating that the time-dependent changes in TER we had previously observed (Fig. 4, A–B) were almost entirely attributable to changes in P_{Na} .

Permeation of Other Alkali Metal Cations—Although Na^+ and Cl^- are the major charge carriers that MDCK cells encounter in cell culture medium and Ringer saline, the native milieu of claudin-8 is the distal renal tubule, which is exposed to high concentrations of K^+ at the luminal surface. To assess the relative permeability of the monolayers to different alkali

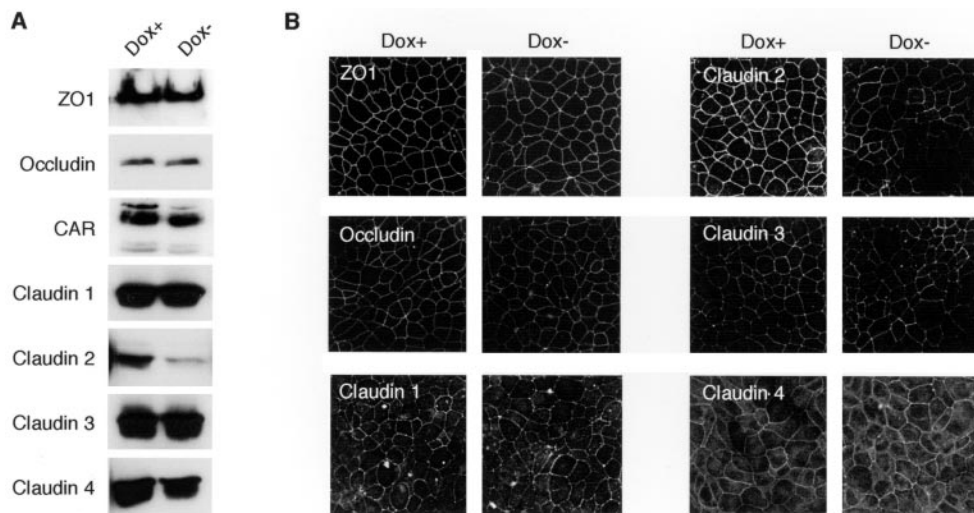
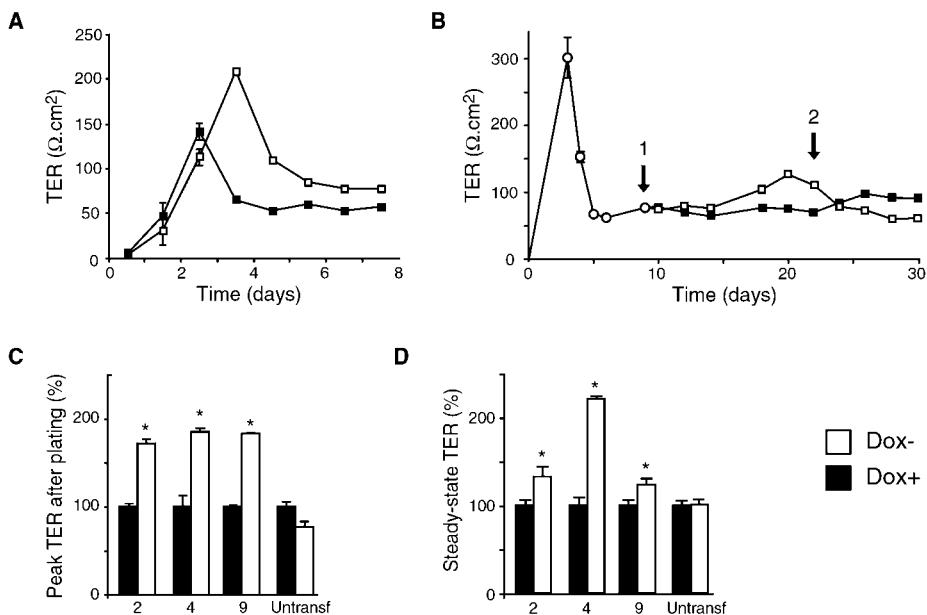


FIG. 3. **Expression of endogenous tight junction proteins in claudin-8 expressing cell lines.** A, Western blots of cells grown in the presence or absence of doxycycline. B, immunofluorescence staining of Dox+ and Dox- cells with antibodies to the indicated tight junction proteins.

FIG. 4. **Effect of claudin-8 expression on TER.** Cells were grown on filters in the absence of doxycycline to induce claudin-8 expression (Dox-; white symbols and columns) or in its presence to suppress claudin-8 expression (Dox+; black symbols and columns). A, cells were plated in the absence or presence of doxycycline on day 0 and followed thereafter. B, cells were all initially plated in the presence of doxycycline. On day 9 (arrow 1) half of the filters (white symbols) were switched to Dox-. On day 22 (arrow 2) the two groups were crossed over so that the other half (black symbols) were deprived of doxycycline. C and D, summary of experiments similar to those in A, performed in all three MDCK II TetOff claudin-8 NFL cell lines (clones 2, 4, and 9) and in untransfected MDCK II TetOff negative control cells (*Untransf*), showing the TER in Dox- cells relative to that in Dox+ cells (normalized to 100%) at the peak of the initial overshoot after plating (C) and at steady state (D). *, $p < 0.05$ for Dox- versus Dox+.



metal cations, the bath solutions were exchanged so that one side was bathed in 150 mM NaCl and the contralateral side was bathed in 150 mM chloride salt of monovalent alkali metal cations. From the biionic potential measured across the monolayer, the relative permeability to Na^+ versus the other cation was then calculated (Table I and Fig. 6A). As has previously been reported, the range of permeabilities of the alkali metal cations is very narrow, suggesting that the permeating pathway is a relatively water-filled pore (31). The order of permeabilities was generally $\text{Na}^+ \sim \text{Li}^+ \sim \text{K}^+ > \text{Rb}^+ \gg \text{Cs}^+$, almost in reverse-order of their free-solution mobilities, and approximated sequences IX through XI of the Eisenman series. This suggests that the paracellular cation permeation pathway has negatively charged binding sites with relatively high affinity for dehydrated monovalent cations (34). Furthermore, the permeability to all of the cations was reduced to the same extent in Dox- compared with Dox+ cells so that the selectivity sequence was unchanged.

In the presence of strong binding sites in a pore, a cation that binds with high affinity would be released slowly from the binding site, and therefore, its conductance across the pore

would be paradoxically low (the so-called “sticky pore problem”) (35). This can give rise to a discrepancy between the relative permeabilities, as determined by diffusion potentials at equilibrium, and the conductance, as determined during the passage of current. We therefore determined the relative conductance of the paracellular pathway for alkali metal cations by measuring transepithelial conductance in the presence of symmetrical 150 mM solutions of the chloride salt of each cation (Fig. 6B). Indeed, the order of conductance, $\text{K}^+ > \text{Rb}^+ > \text{Na}^+ > \text{Cs}^+ > \text{Li}^+$ (Eisenman V), was quite different from the order of permeabilities and suggests that small cations with a strong electrostatic interaction with the paracellular pore such as Li^+ and Na^+ may bind so tightly as to impede their conductance. Importantly though, the relative conductance was also no different between Dox- and Dox+ cells, suggesting that claudin-8 expression does not induce any drastic differences in either the cation binding site or the pore structure of the paracellular pathway.

Permeation of Organic Monovalent Cations—To probe the size selectivity of the paracellular pore, similar biionic potential and conductance measurements were performed with a

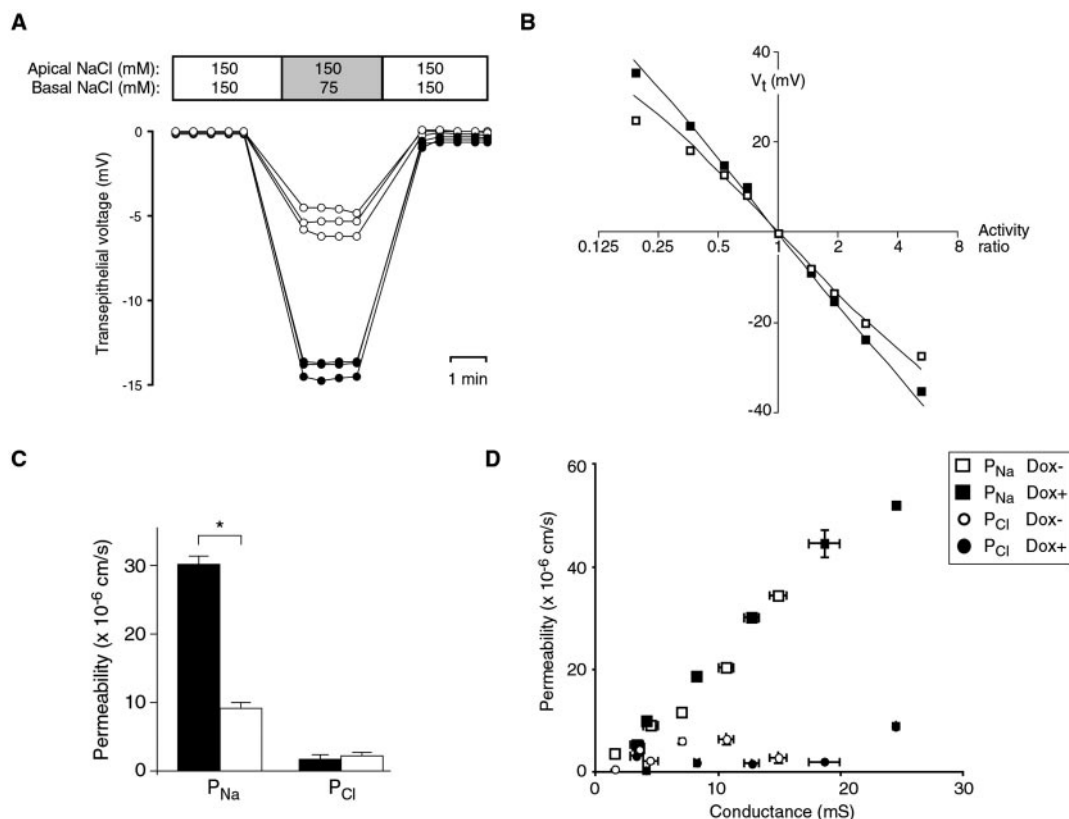


FIG. 5. Determination of NaCl permeability from conductance and dilution potential measurements. *A*, representative voltage traces from three Dox⁻ (white symbols) and three Dox⁺ (black symbols) epithelial monolayers acquired simultaneously in Ussing chambers under a zero-current clamp. For the sake of clarity only data points at 30-s intervals are shown. The dilution potential was determined from the change in transepithelial voltage upon switching from symmetrical bathing solutions to a 2:1 NaCl concentration gradient. *B*, NaCl dilution potentials conform to the Goldman-Hodgkin-Katz equation. The data points represent dilution potentials (V_t) experimentally determined in a single monolayer bathed in asymmetrical NaCl solutions. The abscissa shows the ratio of NaCl activity in apical compared with basal compartments (α). The curves were fitted by nonlinear regression to the equation $V_t = -RT/F \ln[(\alpha + \beta)/(1 + \alpha\beta)]$, using values of β of 0.14 (Dox⁻) and 0.05 (Dox⁺). *C*, typical values of P_{Na} and P_{Cl} from a single experiment performed on three Dox⁻ (white columns) and three Dox⁺ (black columns) monolayers. *, $p < 0.0005$. *D*, summary of data from individual experiments performed at six different time points after plating, showing the extracted values of P_{Na} and P_{Cl} plotted as a function of total conductance. Each data point represents the mean \pm S.E. of three monolayers; the key to symbols is on the far right panel.

TABLE I
Relative permeability of monovalent cations as determined from bilonic potentials

| | M_r | Mean diameter ^a | P_x/P_{Na} | |
|----------------------|-------|----------------------------|------------------|------------------|
| | | | Dox ⁻ | Dox ⁺ |
| | | Å | | |
| Li ⁺ | 7 | 1.20 | 0.99 \pm 0.01 | 0.97 \pm 0.00 |
| Na ⁺ | 23 | 1.90 | 1.00 | |
| K ⁺ | 39 | 2.66 | 0.95 \pm 0.01 | 0.97 \pm 0.01 |
| Rb ⁺ | 85 | 2.96 | 0.84 \pm 0.00 | 0.86 \pm 0.00 |
| Cs ⁺ | 133 | 3.38 | 0.66 \pm 0.02 | 0.68 \pm 0.00 |
| Methylamine | 32 | 3.78 | 0.67 \pm 0.02 | 0.66 \pm 0.02 |
| Ethylamine | 46 | 4.58 | 0.33 \pm 0.03 | 0.35 \pm 0.01 |
| Guanidine | 60 | 4.44 | 0.72 \pm 0.02 | 0.67 \pm 0.01 |
| Tetramethylammonium | 75 | 5.50 | 0.36 \pm 0.09 | 0.26 \pm 0.07 |
| Dimethylethanolamine | 90 | 5.47 | 0.22 \pm 0.04 | 0.18 \pm 0.01 |
| Choline | 104 | 6.02 | 0.21 \pm 0.04 | 0.15 \pm 0.01 |
| Tetraethylammonium | 130 | 6.58 | 0.38 \pm 0.08 | 0.27 \pm 0.06 |
| Lysine | 147 | 6.78 | 0.36 \pm 0.06 | 0.24 \pm 0.01 |
| Arginine | 175 | 6.96 | 0.24 \pm 0.03 | 0.16 \pm 0.01 |
| N-Methyl-D-glucamine | 195 | 7.29 | 0.42 \pm 0.05 | 0.26 \pm 0.06 |

^a The mean diameter of the alkali metal cations is defined as twice the Pauling radius of the nonhydrated ion. The mean diameter of the organic cations, derived from the data of Dwyer *et al.* (28), is defined as the geometric mean of the dimensions of a rectangular box that would contain the ion as determined using Corey-Pauling-Koltum space-filling molecular models.

range of monovalent organic cations of varying sizes (Table I and Fig. 6, *C* and *D*). Although the data show the expected monotonic decrease in permeability with increasing ionic diameter within the range 3.8 to 7.3 Å, there is considerable scatter, as has been observed in similar studies done on gallbladder epithelium (36) and muscle end-plate Na⁺ channels (28), indi-

cating that nitrogenous cations are imperfect probes of pore size. Part of the size-independent variation in permeation through the paracellular pathway in gallbladder epithelium could be attributed to differences in hydrogen-bonding capability of the cation, which determines its interaction with partial negative charges in the paracellular pore (36). Consistent with

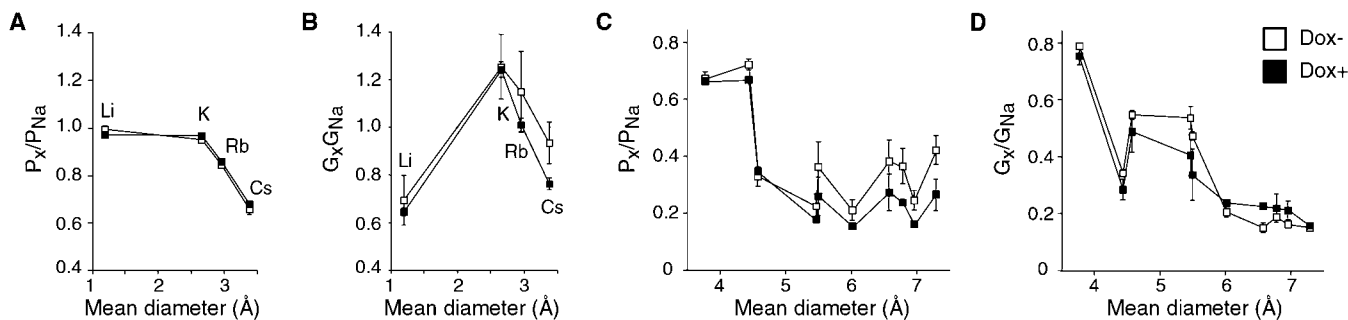


FIG. 6. **Relative permeability and conductance of monovalent cations.** *A*, permeability of alkali metal cations relative to Na^+ , as determined by biionic potential measurements. *B*, conductance of alkali metal cations relative to Na^+ . The dashed line in each panel represents permeability/conductance identical to that of Na^+ . *C*, permeability of organic cations relative to Na^+ . *D*, conductance of organic cations relative to Na^+ .

this, we find anomalously high permeabilities and, as might be predicted, low conductances for compounds with multiple protons available for hydrogen-bonding such as guanidine and *N*-methyl-D-glucamine (Table I).

Because many of the nitrogenous cations used are quite lipophilic, errors could arise either due to permeation of the neutral form of the organic cation across the lipid bilayer, which might significantly reduce the protonated form at the unstirred layer, or even due to permeation of a charged form that is sufficiently lipophilic to cross the lipid bilayer (37). We believe this is unlikely for three reasons. First, we chose cations with a $\text{p}K_a > 9$, so that less than 1% would be deprotonated at pH 7.4. Second, permeabilities tended to be higher for ions with greater hydrogen-bonding capability, the opposite of what would be expected for lipid permeation. Third, extensive studies performed by Moreno and Diamond (36) clearly demonstrate that lipid permeation of such compounds was negligible compared with paracellular permeation in the gallbladder, a leaky epithelium with many similarities in its paracellular permeability properties to MDCK II.

Importantly, the permeability of all the cations tested relative to P_{Na} was no different between Dox⁻ and Dox⁺ cells. Because we have already shown that P_{Na} is markedly decreased in Dox⁻ cells, this indicates that the absolute permeabilities to the other cations were all decreased proportionately. This again suggests that the physical structure of the paracellular pore, including its apparent diameter, has not been drastically altered.

Permeation of Divalent Cations and Neutral Solutes—Radio-tracer flux studies were next used to determine the permeability of the monolayers to calcium. Electrophysiological studies were not used because they would entail exposure of the monolayers to large alterations in the concentration of calcium that could potentially affect tight junction integrity and intracellular signaling processes. As shown in Fig. 7, MDCK II monolayers are quite permeable to calcium, and this permeability was reduced by almost 3-fold by claudin-8 expression in Dox⁻ cells. In a set of matched monolayers that were assayed simultaneously for calcium permeability by tracer flux and Na^+ permeability by dilution potential, $P_{\text{Ca}}/P_{\text{Na}}$ was found to be exactly the same in Dox⁻ (4.41 ± 0.11) and Dox⁺ (4.49 ± 0.11) cells. If claudin-8 decreased paracellular cation permeability by altering charge distribution in or around the paracellular pore, this should have a disproportionately greater effect on permeation of multivalent compared with monovalent ions. The striking finding that divalent cation permeability is reduced to a degree exactly proportionate to the change in P_{Na} argues strongly against an electrostatic effect of claudin-8. By contrast, the permeability to neutral solutes, as inferred from the measurement of radiolabeled mannitol and urea fluxes, was no different between Dox⁻ and Dox⁺ cells (Fig. 7).

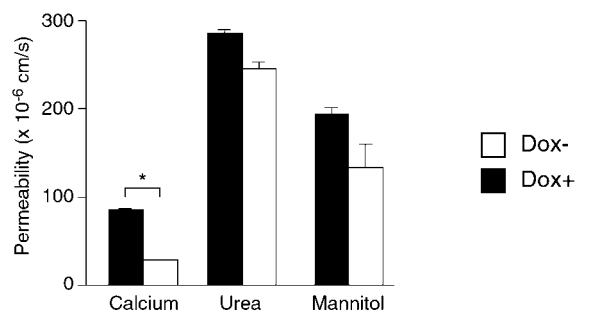


FIG. 7. **Permeabilities of divalent cations and neutral solutes determined from radioactive tracer fluxes.** White bars, Dox⁻; black bars, Dox⁺. *, $p < 0.00005$.

Temperature Dependence of Na^+ Permeation—If claudin-8 expression in some way impedes cation permeation across paracellular pores, the activation energy for Na^+ permeation should be increased. To test this, the transmonolayer conductance in Ringer solution, which we have shown is dominated by the Na^+ conductance, and P_{Na} determined from dilution potentials were measured at different temperatures, and molar activation energies were derived from Arrhenius plots (Fig. 8). As expected, the activation energy for total conductance and P_{Na} were very similar, likely indicating that they both reflect the energy barrier to Na^+ permeation. The values obtained were quite low and in the same range as that observed for transmembrane ion channels (38). Importantly, the activation energy was unchanged by claudin-8 expression, indicating that whatever the mechanism by which claudin-8 reduces Na^+ conductance, it is not by inducing an unfavorable energetic landscape.

DISCUSSION

Methodologic Issues—We describe herein a novel cell line with overexpression of claudin-8. The levels of expression of the heterologous protein appear to be relatively modest because we were able to detect it by Western blotting only in enriched membrane fractions. We attribute this to our use of a retroviral vector, which generally leads to a high percentage of stably transfected cells but a low number of integrated transgene copies per cell. The inadvertent use of a low copy number technique may account for two potential advantages of our study over some prior ones. First, there was no detectable “leakage” of expression in the suppressed (Dox⁺) state. Second, expression of claudin-8 generated very few additional and/or aberrant tight junction strands. A recent study of claudin-1 suggests that excessively high levels of claudin overexpression may be responsible for inducing aberrant strands and that these aberrant strands lack normal tight junction components such as occludin (39). To the extent that such strands are

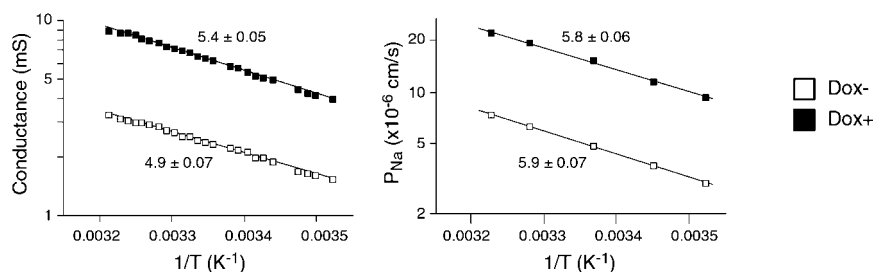


FIG. 8. Arrhenius plots to show the temperature dependence of paracellular permeability to Na^+ . The ordinate represents on a logarithmic scale the transepithelial conductance (left panel) and P_{Na} determined by measuring the NaCl dilution potential (right panel) in Dox- (white squares) and Dox+ (black squares) monolayers. The abscissa represents the reciprocal of the absolute temperature. The lines were obtained by fitting the data by nonlinear regression to the equation, $\ln(y) = \ln(K) - E_a/RT$, where y is the ordinate variable, and K is a pre-exponential constant. The estimates for the activation energy, E_a (kcal/mol; mean \pm S.E.), are shown next to each line.

non-physiological, their presence is undesirable and may complicate interpretation of claudin expression studies.

The transgene we used encodes an N-terminal FLAG epitope-tagged claudin-8 protein. We do not believe that the epitope tag interfered with claudin-8 function for three reasons. First, claudin-8 was appropriately targeted to the tight junction. Second, other studies report that epitope-tagged claudin constructs (of the C terminus) are still able to form *de novo* tight junctions and mediate adhesion in fibroblasts (40) and, when expressed at low levels, incorporate into existing tight junction strands (39). Third, we tagged the N terminus rather than the C terminus, which encodes a PDZ binding motif (41), to eliminate the potential for interference with binding to the PDZ domains of ZO-1, -2, and -3. Nevertheless, we cannot exclude completely the possibility that an N-terminal tag may allow appropriate incorporation into the tight junction but interferes in some subtle way with the permeability properties of the protein.

We assessed the level of expression and localization of other tight junction components for which reagents were available, including claudins 1–4, ZO-1, and occludin and found no change with induction of claudin-8 expression, except for a reduction in the expression level of claudin-2. The fact that only claudin-2 was affected might argue against a nonspecific effect of claudin-8 overexpression on tight junction assembly or integrity. The possibility that other claudin isoforms that were not tested for are expressed in MDCK II cells and might be affected by claudin-8 overexpression cannot be ruled out.

General Properties of Paracellular Permeation in MDCK II Cells—In our studies, the native paracellular pathway in MDCK II cells was found to be highly cation-selective, exhibited an alkali cation selectivity for permeability consistent with strong electrostatic interaction between pore and permeating cation, showed substantial discrepancies between permeability and conductance selectivity, favored organic cations with strong hydrogen-bonding capability, and exhibited an activation energy of permeation that was very low and in the range observed for transmembrane ion channels. These findings are consistent with the model developed by Diamond and co-workers (33, 36, 42) based on a series of comprehensive studies in gallbladder epithelium, which also has a leaky cation-selective paracellular permeability resembling that of MDCK II cells. In this model, the paracellular pathway behaves as a series of relatively wide, water-filled pores or channels lined by residues with polarizable negative charges available for binding to permeating cations.

Functional Consequences of Claudin-8 Overexpression—The principal finding of this study is that overexpression of claudin-8 leads to a reduction in paracellular permeability to Na^+ and other cations but not to anions or neutral solutes. In simple

terms, there are three ways in which a reduction in ion permeability can be effected. First, the size of the paracellular pore may be reduced or its shape altered in such a way as to sterically hinder Na^+ permeation. Second, electrostatic interactions between the permeating Na^+ ion and the pore may be altered. Such interactions may occur with residues that bear overall net charge or with charged side groups of residues or with polarizable moieties and include both surface charge effects and direct interactions inside the pore. Third, the physicochemical nature of the pores may be unchanged, but the number of functioning pores may be reduced either because of a reduction in the total number of pore protein molecules present or because some of the pores become closed (if this is possible).

Our finding that the size selectivity of the pore to organic cations varying in size from 3.8 to 7.3 Å is unaltered argues against the first possibility. Our finding that the relative permeability among different alkali metal ions is unchanged and that permeability to monovalent and divalent cations is proportionately reduced argues against the second possibility. Moreover, both of the first two hypotheses are ruled out by our observation that the activation energy for Na^+ permeation is unchanged. Thus, purely from physiological observations, we are led to the only possible conclusion, that claudin-8 must somehow reduce the number of functioning Na^+ -permeable pores.

Difficulty in Interpreting Claudin Overexpression Studies—The extrapolation of the properties of individual claudins from the phenotype of transfected cell lines reported in the literature has been problematic for a variety of reasons. First, it is uncertain whether the overexpressed claudin inserts new pores into existing tight junction strands or contributes structural building blocks to augment the paracellular barrier. In some studies overexpression of claudin increases permeability (22, 23), whereas in others it decreases it (18–20). A second problem in interpreting transfection studies is that it is usually not known whether the overexpressed claudin is added to existing tight junction components or substituting for a component that then becomes down-regulated. Because of the lack of availability of antibodies, it is not yet possible to measure all of the claudins that are currently known, and of course other as-yet unidentified claudins or other tight junction membrane proteins cannot be accounted for at all. Third, the tight junction strand permeability may be dependent not only on the presence or absence of a particular claudin but also on the presence or absence of other non-pore-forming “structural” components of the strand. For example, it is not difficult to imagine that the permeability of a normal tight junction strand containing claudin-1 might be quite different from that of an aberrant strand containing claudin-1 but lacking occludin (as found by McCarthy (19)). Finally, each pore may not necessarily be formed

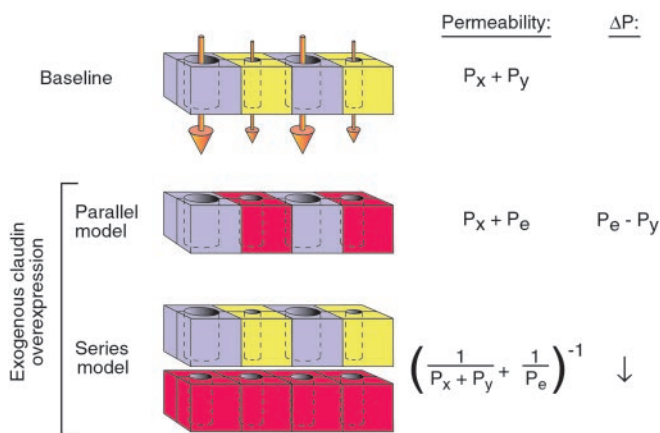


FIG. 9. Models for how exogenously overexpressed claudins might incorporate into native tight junctions. Tight junction strands are depicted as continuous strings of paired claudin molecules. The two apposed molecules of each pair derive from the lateral membrane of the two adjacent cells. Solutes and water (arrows) can pass through pores in the claudin dimers. Different isoforms of claudins have different pore permeabilities (purple, P_x ; yellow, P_y). The base-line permeability of a single native tight junction strand to any given solute is the sum of the permeabilities of these different pores ($P_x + P_y$). Exogenously overexpressed claudins generate pore-forming protein pairs (red) with permeability, P_e . The total permeability of the resultant junction and the possible direction(s) for the change in permeability from baseline (ΔP) are shown in the columns to the right of each model. *Parallel model*, exogenous claudins replace endogenous claudins, resulting in a new set of pores in parallel with pre-existing ones. The total permeability may increase (if $P_e > P_y$) or decrease (if $P_e < P_y$). *Series model*, exogenous claudins form new strands in series with pre-existing strands, decreasing total permeability.

by the molecules of a single claudin isoform. Tsukita and co-workers (40) show that different claudin isoforms can adhere from cell to cell in a heterotypic manner and associate within a strand into heteropolymers. If each pore is lined by multiple claudin molecules, it is conceivable that the permeability properties of that pore may be dependent on the particular combination of claudin isoforms that are present.

A Model to Explain the Consequences of Claudin Overexpression—As a first step toward interpreting claudin overexpression studies, we propose a simple model (Fig. 9). We assume that claudins are homotypically associated pore-forming proteins and ignore for the sake of simplicity the possibility of pores formed by heterotypic interactions. Claudins are depicted as dimers, but the actual stoichiometry is currently unknown. We also assume that a finite number of proteins is packed into a mature tight junction strand to form a continuous seal. Therefore, each overexpressed claudin molecule must either displace an existing tight junction protein or incorporate in a whole new tight junction strand. In our models, claudins can have permeabilities that range from very high to negligibly low. The latter are indistinguishable from tight junction proteins that have no pores and purely exist to complete the barrier (“barrier proteins”). We propose two simple scenarios upon exogenous claudin overexpression. The new claudin molecules may substitute for endogenous tight junction proteins on the same strand (parallel model) or assemble into new tight junction strands in series with existing ones (series model). Although it might be assumed that the change in permeability upon overexpression of a single claudin isoform is a direct measure of the permeability of that isoform (*i.e.* that $\Delta P = P_e$), our model clearly shows that this is true only in the specific situation in which exogenous claudin incorporates in a parallel fashion (*i.e.* no change in strand number) and replaces a barrier protein (*i.e.* $P_y = 0$). No reported studies so far unequivocally fulfil these criteria.

The studies of McCarthy *et al.* (19), van Itallie *et al.* (20), and Colegio *et al.* (21), in which ion permeability is reduced concurrent with the appearance of aberrant strands, can now be seen to be most consistent with the series model. The overexpression of claudin-2 by Furuse *et al.* (22), in which permeability is increased without any apparent change in tight junction strands, is consistent with a parallel model, in which a less permeable tight junction component is replaced by the more permeable claudin-2. In the current study, our finding of decreased cation permeability without a substantive change in strand number can only be explained by the parallel model. Indeed, our detailed physiological characterization strongly suggests that a cation-permeable claudin was replaced by claudin-8, which must itself be relatively or absolutely impermeable to Na^+ and other cations. A recent study demonstrated that claudin-2 overexpression increased cation permeability in MDCK cells of high transepithelial resistance, suggesting that claudin-2 is a paracellular cation channel (23). Given that the expression of claudin-2 in our cell lines is substantially reduced, we speculate that its replacement by claudin-8 accounts for all of the observed phenotypic findings. We conclude that claudin-8 acts as a nonspecific cation barrier and suggest that it may play an important role in maintaining transtubular cation gradients in the distal renal tubule.

Acknowledgments—We thank Joanne M. McCormack for technical support, Brad Denker for sharing equipment and stock cell lines, Christopher Cohen for providing coxsackie- and adenovirus-associated receptor antisera, Michelle MacVeigh for confocal microscopy assistance, and Joe Mindell for helpful discussions.

REFERENCES

- Denker, B. M., and Nigam, S. K. (1998) *Am. J. Physiol.* **274**, F1–F9
- Fanning, A. S., Mitic, L. L., and Anderson, J. M. (1999) *J. Am. Soc. Nephrol.* **10**, 1337–1345
- Furuse, M., Hirase, T., Itoh, M., Nagafuchi, A., Yonemura, S., Tsukita, S., and Tsukita, S. (1993) *J. Cell Biol.* **123**, 1777–1788
- Martin-Padura, I., Lostaglio, S., Schneemann, M., Williams, L., Romano, M., Fruscella, P., Panzeri, C., Stoppacciaro, A., Ruco, L., Villa, A., Simmons, D., and Dejana, E. (1998) *J. Cell Biol.* **142**, 117–127
- Cunningham, S. A., Arrate, M. P., Rodriguez, J. M., Bjerkner, R. J., Vanderslice, P., Morris, A. P., and Brock, T. A. (2000) *J. Biol. Chem.* **275**, 34750–34756
- Cohen, C. J., Shieh, J. T., Pickles, R. J., Okegawa, T., Hsieh, J. T., and Bergelson, J. M. (2001) *Proc. Natl. Acad. Sci. U. S. A.* **98**, 15191–15196
- Nasdala, I., Wolburg-Buchholz, K., Wolburg, H., Kuhn, A., Ebnet, K., Brachtendorf, G., Samulowitz, U., Kuster, B., Engelhardt, B., Vestweber, D., and Butz, S. (2002) *J. Biol. Chem.* **277**, 16294–16303
- Furuse, M., Sasaki, H., Fujimoto, K., and Tsukita, S. (1998) *J. Cell Biol.* **143**, 391–401
- Tsukita, S., and Furuse, M. (2000) *J. Cell Biol.* **149**, 13–16
- Rahner, C., Mitic, L. L., and Anderson, J. M. (2001) *Gastroenterology* **120**, 411–422
- Yu, A., and Enck, A. (2001) *J. Am. Soc. Nephrol.* **12**, 45 (abstr.)
- Kiuchi-Saishin, Y., Gotoh, S., Furuse, M., Takasuga, A., Tano, Y., and Tsukita, S. (2002) *J. Am. Soc. Nephrol.* **13**, 875–886
- Reyes, J. L., Lamas, M., Martin, D., Del Carmen Namorado, M., Islas, S., Luna, J., Tauc, M., and Gonzalez-Mariscal, L. (2002) *Kidney Int.* **62**, 476–487
- Simon, D. B., Lu, Y., Choate, K. A., Velazquez, H., Al-Sabban, E., Praga, M., Casari, G., Bettinelli, A., Colussi, G., Rodriguez-Soriano, J., McCredie, D., Milford, D., Sanjad, S., and Lifton, R. P. (1999) *Science* **285**, 103–106
- Lu, Y., Choate, K. A., Wang, T., and Lifton, R. P. (2001) *J. Am. Soc. Nephrol.* **12**, 756 (abstr.)
- Furuse, M., Hata, M., Furuse, K., Yoshida, Y., Haratake, A., Sugitani, Y., Noda, T., Kubo, A., and Tsukita, S. (2002) *J. Cell Biol.* **156**, 1099–1111
- Turksen, K., and Troy, T. C. (2002) *Development* **129**, 1775–1784
- Inai, T., Kobayashi, J., and Shibata, Y. (1999) *Eur. J. Cell Biol.* **78**, 849–855
- McCarthy, K. M., Francis, S. A., McCormack, J. M., Lai, J., Rogers, R. A., Skare, I. B., Lynch, R. D., and Schneeberger, E. E. (2000) *J. Cell Sci.* **113**, 3387–3398
- Van Itallie, C., Rahner, C., and Anderson, J. M. (2001) *J. Clin. Invest.* **107**, 1319–1327
- Colegio, O. R., Van Itallie, C. M., McCrea, H. J., Rahner, C., and Anderson, J. M. (2002) *Am. J. Physiol. Cell Physiol.* **283**, 142–147
- Furuse, M., Furuse, K., Sasaki, H., and Tsukita, S. (2001) *J. Cell Biol.* **153**, 263–272
- Amasheh, S., Meiri, N., Gitter, A. H., Schoneberg, T., Mankertz, J., Schulzke, J. D., and Fromm, M. (2002) *J. Cell Sci.* **115**, 4969–4976
- Dowland, L. K., Luyckx, V. A., Enck, A. H., Leclercq, B., and Yu, A. S. L. (2000) *J. Biol. Chem.* **275**, 37765–37773
- Morita, K., Furuse, M., Fujimoto, K., and Tsukita, S. (1999) *Proc. Natl. Acad. Sci. U. S. A.* **96**, 5111–5116
- McCarthy, K. M., Skare, I. B., and Stankewich, M. C. (1996) *J. Cell Sci.* **109**,

2287–2298

27. Wedner, H. J., and Diamond, J. M. (1969) *J. Membr. Biol.* **1**, 92–108
28. Dwyer, T. M., Adams, D. J., and Hille, B. (1980) *J. Gen. Physiol.* **75**, 469–492
29. Barry, P. H., and Diamond, J. M. (1970) *J. Membr. Biol.* **3**, 93–122
30. Kimizuka, H., and Koketsu, K. (1964) *J. Theor. Biol.* **6**, 290–305
31. Cereijido, M., Robbins, E. S., Dolan, W. J., Rotunno, C. A., and Sabatini, D. D. (1978) *J. Cell Biol.* **77**, 853–880
32. Misfeldt, D. S., Hamamoto, S. T., and Pitelka, D. R. (1976) *Proc. Natl. Acad. Sci. U. S. A.* **73**, 1212–1216
33. Barry, P. H., Diamond, J. M., and Wright, E. M. (1971) *J. Membr. Biol.* **4**, 358–394
34. Diamond, J. M., and Wright, E. M. (1969) *Annu. Rev. Physiol.* **31**, 581–646
35. McCleskey, E. W. (1999) *J. Gen. Physiol.* **113**, 765–772
36. Moreno, J. H., and Diamond, J. M. (1975) *J. Membr. Biol.* **21**, 197–259
37. Finkelstein, A. (1970) *Biochim. Biophys. Acta* **205**, 1–6
38. DeCoursey, T. E., and Cherny, V. V. (1998) *J. Gen. Physiol.* **112**, 503–522
39. Kobayashi, J., Inai, T., and Shibata, Y. (2002) *Histochem. Cell Biol.* **117**, 29–39
40. Furuse, M., Sasaki, H., and Tsukita, S. (1999) *J. Cell Biol.* **147**, 891–903
41. Itoh, M., Furuse, M., Morita, K., Kubota, K., Saitou, M., and Tsukita, S. (1999) *J. Cell Biol.* **147**, 1351–1363
42. Wright, E. M., Barry, P. H., and Diamond, J. M. (1971) *J. Membr. Biol.* **4**, 331–357